Fourier-limited Raman velocimetry of laser-cooled, polarized, cesium atoms

Julien Chabé, Hans Lignier, Pascal Szriftgiser, Jean Claude Garreau

Fourier-limited Raman velocimetry of laser-cooled, polarized, cesium atoms

Julien Chabé, Hans Lignier,* Pascal Szriftgiser, and Jean Claude Garreau
Laboratoire de Physique des Lasers, Atomes et Molécules,
UMR CNRS 8523, Centre d'Études et de Recherches Laser et Applications,
Université des Sciences et Technologies de Lille, F-59655 Villeneuve d'Ascq Cedex, France†
(Dated: 23 March 2006)

We describe and test experimentally a setup allowing efficient optical pumping of laser-cooled cesium atoms into the $F = 4$, $m_4 = 0$ ground-state Zeeman sublevel, which is insensitive to magnetic perturbations. High resolution Raman stimulated spectroscopy is shown to produce Fourier-limited lines, allowing, in realistic experimental conditions, atomic velocity selection to one-fifth of a recoil velocity.

PACS numbers: 42.50.Vk, 32.80.Pj, 32.60.+i

I. INTRODUCTION

Raman stimulated spectroscopy has been in one of the most fertile techniques used for manipulating laser-cooled atoms. It has been used for atomic velocity selection [1], sub-recoil laser cooling [2, 3] or quantum state preparation and detection [4, 5], with applications in as different fields as quantum chaos [6], quantum information processing [7] and high-precision metrology of fundamental constants [8]. Being a *stimulated* two-photon transition between two ground-state hyperfine sublevels, the width of the Raman transition is, in principle, limited only by the duration of interaction between the atom and the light (the Fourier limit), as no natural widths are involved in the process. However, for most usual atomic species used in laser cooling (e.g. alkaline and alkaline-earths), the ground state presents hyperfine Zeeman sublevels, so that Zeeman effect and radiation induced light-shifts inhomogeneously broaden the Raman transition. Even if fluctuations of the environmental magnetic field are shielded [9], residual magnetic fields are still of the order of a fraction of mG. For cesium, this correspond to a linewidth of about 1 kHz, or $v_r/8$ where $v_r = \hbar k_L/M$ is the so-called recoil velocity ($k_L = 2\pi/\lambda_L$ being the wave number of the radiation), to which one must add the effect of light-shift fluctuations. A solution to obtain sharper lines is to pump the atoms into a particular sublevel, to avoid inhomogeneous broadening due to the different Zeeman- and light-shifts couplings of the various sublevels. Pumping the atoms into the $m_F = 0$ Zeeman sublevel [10] is even more interesting, as this level is not affected by the magnetic field at all. We have previously identified light-shift fluctuations as an important source of inhomogeneous broadening [11], because usual Raman beam configurations produce different light-shifts for different Zeeman sublevels. Hence, putting all atoms in the same Zeeman sublevel also reduces this effect.

In the present work we describe a setup allowing to perform optical pumping of laser-cooled cesium atoms into the $F = 4$, $m_4 = 0$ ground-state hyperfine sublevel. The method we use here has been previously described by Avila *et al.* [12], for a beam of (hot) cesium atoms. The particularity of the present work is that it concentrates on the improvement of the sensitivity of the Raman velocimetry technique (RV) thanks to the atomic polarization. RV also allows to precisely measure the heating of the atoms by the polarization process itself, a parameter that is of obviously importance when dealing with laser-cooled atoms. We achieve a degree of polarization higher than 75 % of the atoms in the $m_4 = 0$ sublevel. The observed Raman transition FWHM is 160 Hz, which corresponds to a velocity resolution of $v_r/50$ (~ 70 μm/s), to be compared to the $v_r/2$ resolution of the best compensated-magnetic-field line we observed in the same atomic setup [11], with unpolarized atoms. Our resolution is Fourier-limited, i.e. the width of the line is close to the inverse of the duration of the Raman pulse, which can be considered as the ultimate resolution limit of Raman spectroscopy.

II. POLARIZATION TECHNIQUE

The linear Zeeman shift of a ground-state hyperfine sublevel of magnetic quantum number m_F in cesium is given by

$$\delta\nu_Z = Z_F m_F B \tag{1}$$

with the Zeeman coefficients $Z_4 \approx 350$ kHz/G and $Z_3 \approx -351$ kHz/G, and B the magnetic field. In the Earth's magnetic field, the ratio of the Zeeman shift between sublevels and the ambient-temperature thermal energy is about 10^{-8}; sublevels are therefore, under usual conditions, equally populated. *polarisation technique* must thus be devised for putting all (or at least the majority) of the atoms in the same Zeeman sublevel. In this section we briefly discuss some basic aspects of atom polarization, taking into account their main limitations which explain our choices. We consider specifically the case of

*Present address: Dipartimento di Fisica "E. Fermi", Università di Pisa, Largo Pontecorvo 3, I-56127 Pisa, Italy
†URL: http://www.phlam.univ-lille1.fr/atfr/cq

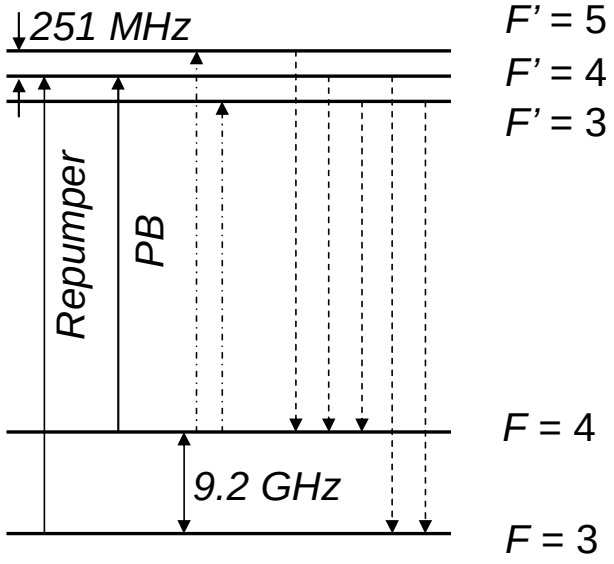

Figure 1: Hyperfine structure of the cesium $6S_{1/2} - 6P_{3/2}$ $D2$ line. The polarizing beam (PB) ($F = 4 \rightarrow F' = 4$) weakly excite stray transitions to the neighbor excited levels $F' = 3, 5$ (cf. text), indicated by dash-dotted arrows. Dashed lines indicate the spontaneous-emission decay channels. The repumper beam brings the atoms "loosen" by decay into the $F = 3$ level back into the optical pumping process (cf. text).

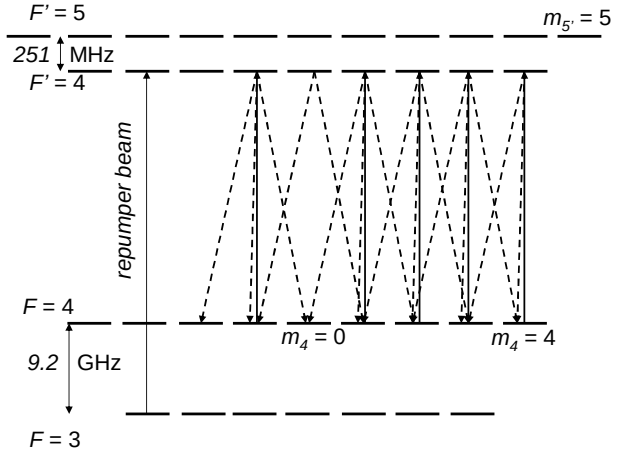

Figure 2: Polarization scheme using optical pumping with π-polarized radiation on a $F \rightarrow F$ transition polarizes the atoms in the magnetic field-insensitive $m_4 = 0$ Zeeman sublevel. Laser-induced transitions are represented by solid arrows, spontaneous transitions by dashed arrows. In order to keep the figure readable, we did not represent all possible transitions.

the cesium atom, although most of our conclusions can be easily extended to most atomic species.

Atomic polarization is usually performed in the presence of a *bias magnetic field*, which has a double purpose: first, it defines a fixed quantization axis for all atoms, and, second, it increases the energy shift of the various Zeeman sublevels in order to prevent a possible reequilibration of level populations by collisions (this last effect is smaller with laser-cooled atoms).

We suppose that all atoms are initially in the $F = 4$ hyperfine sublevel, which is usually the case when they are issued of a magneto-optical trap. The simplest polarizing technique consists in applying a circularly polarized radiation, e.g. a σ^+ beam (with respect to the bias magnetic field), resonant with the $F = 4 \rightarrow F' = 5$ transition (for which the Clebsch-Gordan coefficient is the strongest). An atom in an arbitrary initial sublevel will perform a series of fluorescence cycles until it arrives in the $m_4 = 4$ sublevel, from which it has nowhere else to go. The atom is thus trapped in this maximum-m_F level. Although the transition is in principle closed, the proximity of the neighbor $F' = 4$ excited level, distant of only $\sim$250 MHz, or roughly 50 Γ ($\Gamma \approx 2\pi \times 5.3$ MHz is the natural width of the excited level) means that a small fraction of the atoms is excited to the $F' = 4$ level, from which they can eventually decay to the $F = 3$ hyperfine sublevel (see Fig. 1). Such an atom is lost for the process, because the large energy interval between the ground-state sublevels $F = 3$ and $F = 4$ (9.2 GHz) prevents it to be excited again. One must therefore, as for magneto-optical traps, use a *repumper beam* coupling e.g. levels $F = 3$ and $F' = 4$ and re-injecting the lost atoms into the polarization process (Fig. 1).

The polarization scheme described above is efficient, but it has a major backdraw: the polarized atom, once it arrives at the terminal $m_4 = 4$ sublevel, keeps performing fluorescence cycles on the $m_4 = 4 \rightarrow m_{5'} = 5$ transition, which produces an important heating due to the spontaneous emission recoil, which is obviously undesirable for ultracold atoms.

This inconvenient can be overcome by working on the $F = 4 \rightarrow F' = 4$ transition. The end level $m_4 = 4$ is then not coupled to a σ^+ radiation because there is no excited sub-level satisfying the selection rule $m_{F'} = m_F + 1$; it is in this case a so-called *dark state*: The atom in the end level does not perform any further fluorescence cycles (except for the small probability that it be non-resonantly excited to the $m_{5'} = 5$ sublevel) and there is no additional heating. The transition is however not closed, as the atoms can spontaneously decay from the excited $F = 4$ level to the $F' = 3$ level, but one can again use a repumper beam. This method is a little bit less efficient, as Clebsch-Gordan coefficients for a $F \rightarrow F$ transition are smaller than those of a $F \rightarrow F + 1$ transition, but even modest diode-laser beams can easily saturate these transitions. This polarization method has been used in connexion with stimulated Raman transitions and laser-cooled atoms e.g. in ref. [13].

The polarization technique we use in the present work, schematically presented in Fig. 2, is based on the fact that the Clebsch-Gordan coefficient coupling the ground state Zeeman sublevel $F, m_F = 0$ to the excited Zeeman sublevel $F, m_{F'} = 0$ vanishes. This means that if one

optically pumps the atom with *linearly polarized light* on the $F = 4 \rightarrow F' = 4$ transition, the $m_4 = 0$ level is a dark state, and thus no submitted to additional to spontaneous emission heating.

III. EXPERIMENTAL SETUP

Our experimental setup consists of a standard magneto-optical trap (MOT), a polarizing beam, a repumper beam (which is the same as for the MOT) and a stimulated Raman spectroscopy setup for detecting individual sublevel populations and measuring velocity distributions. The transitions involved in the polarization process are indicated in Fig. 1, and Fig. 3 displays the arrangement of laser beams around the cold-atom cloud.

The bias magnetic field (which defines the quantization axis) is generated by an independent pair of Helmholtz-configured coils. The polarizing beam (PB) is extracted from the same diode laser that produces the MOT beams. The beam is sent through an independent acousto-optical modulator that controls its frequency. The PB is injected in a fiber laser and transported to the region where it interacts with the atom cloud, where it goes through a polarizing cube whose polarization axis is parallel to the bias magnetic field. After interacting with the cloud, the PB is reflected back on the cloud by a mirror. This not only increases the efficiency of the interaction but also prevents the atoms to be pushed out of the axis of the setup by the radiation pressure. The typical incident power on the atom cloud is 2.5 μW. The repumper beam is the same as the MOT repumper. It is formed by three orthogonal, back-reflected laser beams, aligned with the MOT arms, and is resonant with the $F = 3 \rightarrow F' = 4$ transition.

The detailed features of our Raman setup have been discussed in previous publications [11, 14]. In short, the Raman beams are obtained by direct current modulation of a diode laser at 4.6 GHz mounted in a extended-cavity configuration [14]. This generates two sidebands (+1 and -1) in the optical spectrum of the laser, separated by 9.2 GHz. The two sidebands, together, account for 50 % of the total optical power. These sidebands are geometrically separated from the main beam by a diffraction grating and each one is used to perform injection-locking of a power slave diode lasers. We obtain in such a way two powerful (∼150 mW), phase-coherent laser beams whose beatnote FWHM is less that 1 Hz, centered around 9.2 GHz, the ground-state hyperfine interval of cesium. The frequency difference can be controlled to the mHz level by changing the modulation frequency. Each of these beams go through a setup of acousto-optical modulators that allow choosing between the counter- or the copropagating beam Raman configuration. They are then injected in optical fibers that bring them to MOT region. Atoms issued from the MOT setup are mostly in the $F = 4$ ground-state hyperfine level; those in the $F = 3$ level are pushed out of the interaction region by a pulse of a resonant beam. The Raman-resonant atoms are transferred by a Raman pulse to the $F = 3$ level and the atoms remaining in the $F = 4$ level are pushed out of the interaction region by another pushing-beam pulse. Atoms in the $F = 3$ level are then optically repumped to the $F = 4$ level where they are excited by frequency-modulated resonant light and their fluorescence is optically detected by a lock-in amplifier. A small number of atoms, not resonant with the Raman transition, are however optically pumped into the $F = 3$ level by the Raman radiation itself (despite its detuning of 140 GHz with respect to the resonance) or by other stray sources (leaks in the PMO beams, etc.), producing a background signal. In order to correct this background, each Raman measurement is followed by a measurement in identical conditions except that a very large Raman detuning (10 MHz) is set, for which there are no Raman-resonant atoms: the resulting signal is thus a direct measure of the background due to the optical pumping. Subtracting the two values gives us a background-corrected signal.

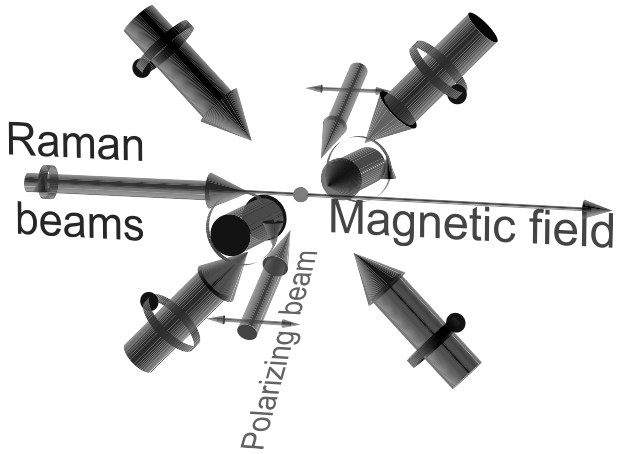

Figure 3: (color online) The atomic cloud and the various lasers beams. Three back-reflected beams are for repumping (large arrows, red in the color version), two σ^+ copropagating Raman beams (thin arrows, orange) – here displayed in the copropagating configuration – induce Raman transitions and the back-reflected polarizing beam (thiner arrows, yellow) whose linear polarization is aligned with the bias magnetic field optically pumps the atoms. The Raman beams are horizontal and aligned with the bias magnetic field where the PB is orthogonal to it, making a 45° angle with respect to the horizontal.

The ambient magnetic field fluctuations are reduced in our setup by an active compensation scheme: small coils with the axis oriented along the three orthogonal directions and located at opposite corners of the cesium-vapor cell measure the magnetic field fluctuations, which are electronically interpolated to deduce the value of the fluctuations in the *center* of the cell. This error signal is used to generate currents sent through 3 mutually orthogonal Helmholtz coil pairs that generate a compensating field. Orthogonally polarized, copropagating, Raman

beams can be used to excite all available Raman lines independently of the atomic velocity, producing a typical linewidth of 3.5 kHz, from which we deduce a residual magnetic field of 300 μG. This linewidth is essentially limited by the residual magnetic field and the Raman beam-induced light shifts, as discussed in detail in ref. [11].

In the present setup, instead of the orthogonal linear polarizations used in [11], both Raman beams are σ^+-polarized. The Raman transition then involves only two Zeeman sublevels $m_F \rightarrow m_F+1 \rightarrow m_F$, so that the intensity of each line in the Raman spectrum, once corrected of the coupling Clebsch-Gordan coefficients, is a direct measurement of the individual sublevel populations [7].

A typical experimental sequence is as follows: the MOT is on for 120 ms, producing an atomic cloud of about 10^8 atoms. The trapping magnetic field is turned off and the MOT beams intensity adiabatically decreased to about $10^{-2}I_s$ (I_s is the saturation intensity $\sim$2.2 mW/cm^2) and the detuning adiabatically changed to $\sim -6\Gamma$, producing a Sisyphus molasses lasting for about 40 ms. This considerably reduces the atomic temperature, leading to a final temperature of 3.2 μK, or a rms velocity of about $4v_r$. The repumper beams are then turned on, as well as the Helmholtz coils that produce the bias field ($\sim$48 mG). One or two pulses of the polarizing beam are applied with user-defined intensity, detuning and duration. The Raman sequence is then used to perform a population measurement. Best results were obtained with two 150 μs-pulses of the PB separated by 250 μs during which the repumper beams are kept on.

IV. RESULTS

A. Polarizing the atoms

In order to measure the effect of polarization, we perform σ^+-polarization Raman stimulated spectroscopy with *copropagating* beams. The transition is then insensitive to the atomic velocity, and the linewidth is due to the finite-duration pulse spectrum and residual perturbations by the magnetic field fluctuations and radiation broadening. The bias magnetic field is adjusted so that lines are clearly separated. Fig. 4 compares the Raman spectra obtained without (a) and with polarization (b). In presence of the PB, 75% of the atoms have been pumped into the $m_4 = 0$ sublevel. The fact that not all atoms are in the dark state can be attributed to experimental imperfections in defining the polarization of the PB beam, due to its transmission through the MOT cell walls at an angle that is not exactly 90°, and to a residual misalignment between the PB polarization and the bias magnetic field, whose direction, moreover, varies a little bit across the atom cloud. Higher polarizations can certainly be obtained, but this would imply, due to the particular geometry of our setup, in an amount of work that is not worth the additional few percent of atoms.

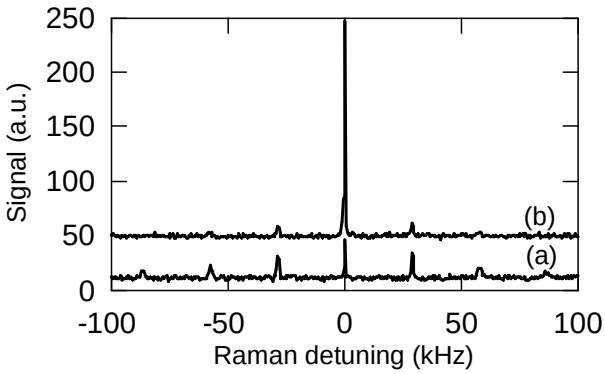

Figure 4: Co-propagating-beam Raman spectra. (a) No polarizing beam applied. (b) Polarizing beam applied (this plot was vertically shifted in order to easy comparison); 75% of the atoms are on the $m_4 = 0$ Zeeman sublevel. The power of the PB is 2.5 μW and its detuning -0.5 Γ.

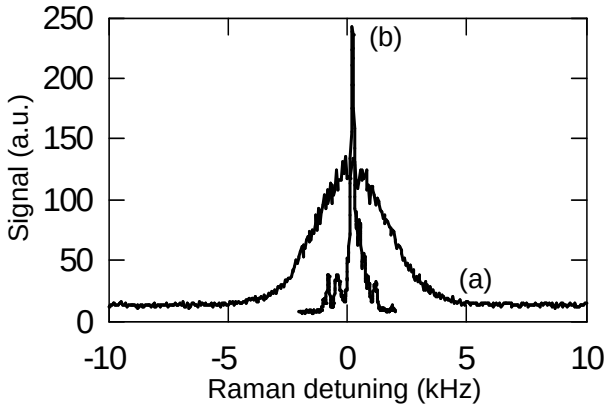

Figure 5: Comparison between (a) the unpolarized Raman line obtained with an actively-compensated magnetic field (3.5 kHz FWHM) and (b) the polarized $m_4 = 0$ line. The FWHM of the polarized line is 160 Hz, which implies a velocity resolution of $v_r/50$.

By comparing the total signal in all lines in the two spectra, we deduce that about 20% of the atoms were lost in the polarization process, which can be attributed essentially to the atom cloud free fall due to gravity.

In order to put into evidence the improvement of our setup due to polarization, we compare in Fig. 5 the unpolarized but magnetic field-compensated line, including contributions from all Zeeman sublevels, and the polarized $m_4 = 0$ line. The observed improvement in the FWHM is 22. The observed width of the polarized line is 160 Hz, which, multiplied by the Raman pulse duration (7 ms) gives 1.12; we are thus very close to the Fourier limit. The structures in the pedestal of the polarized line are generated by weak $m_4 = 0 \rightarrow m_3 = \pm 1$ and

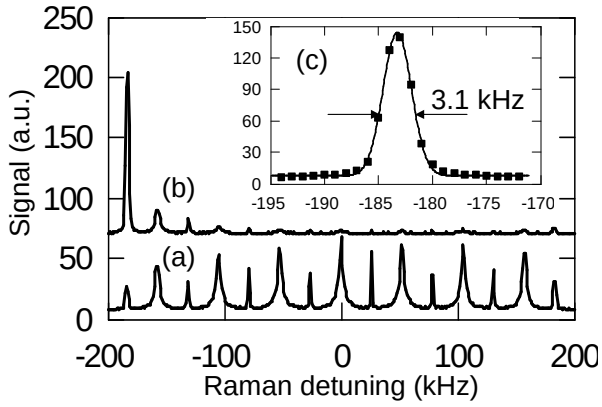

Figure 6: Polarization in the $m_4 = -4$ level with σ^- light on the $F = 4 \rightarrow F' = 4$ transition. The Raman transitions are induced here by orthogonal linearly-polarized beams. Spectrum (a) is without polarizing beam. The spectrum (b) with polarizing beam has been shifted upward in order to easy comparison. The inset (c) shows a zoom on the $m_4 = -4$ line, displaying a FWHM of 3.1 kHz, about 20 times that of the polarized $m_4 = 0$ line shown in Fig. 5.

$m_4 = \pm 1 \rightarrow m_3 = 0$ transitions due to the fact that the Raman beams wavevectors are not perfectly aligned with the bias magnetic field.

For the sake of comparison, we display in Fig. 6 the spectrum obtained by polarizing the atoms into the $m_4 = -4$ level with a σ^- radiation. One cannot, in the present case, use a σ^+ Raman polarization, as it does not allow measuring the $m = -4$ level population, because the end level of the Raman transition would be in such case the inexistent $F = 3, m_3 = 4$ level. We thus used Raman beams with orthogonal linear polarizations, which produces 15 distinct lines mixing different degenerate transitions (see [11] for details). The degree of polarization is of the same order as above ($\sim$75 %) but the resulting polarized line [see inset (c) in Fig. 6] is considerably larger, by a factor of about 20. We clearly see the advantage of pumping the atoms into a $m = 0$ sublevel.

B. Raman velocimetry and heating

As we discussed in sec. II, the fluorescence cycles performed by the atom during the polarization process inevitably induce some spontaneous emission heating. In order to evaluated this heating effect, we compared the lines obtained obtained with *counterpropagating* Raman beams with and without polarization. In the counterpropagating configuration, the transition amplitude depends on the velocity of the atoms via the Doppler effect, and the Raman resonance conditions is:

$$\delta_R = (\omega_2 - \omega_1 - \omega_{hf}) - 2k_L v - 2\omega_r \qquad (2)$$

where $\omega_{1,2}$ are the frequency of the Raman beams, $\omega_{hf} =$ 9.2 GHz is the hyperfine splitting, $k_L = k_1 \approx -k_2$ the wavenumber of the Raman beams, v the atomic velocity and $\omega_r = \hbar k_L^2/(2M)$ is the recoil frequency ($\omega_r \sim 2\pi \times 2$ kHz). The observed width of 160 Hz in the polarized case corresponds to a velocity resolution of $\sim 0.02 v_r$, to be compared to $\sim 0.4 v_r$ in the nonpolarized case.

Δ_{PB}/Γ	τ (ms)	P (μW)	FWHM (kHz)	v_{rms}/v_r
-1.0	0.53	2.41	98.6	5.2
-0.5	0.32	2.34	91.3	4.8
0.0	0.65	2.36	99.6	5.2
No PB	–	–	75.3	4.0

Table I: Heating effect of the polarization process. The duration is chosen so that 50% of the atoms are pumped into the $m_4 = 0$ level. Parameters are the detuning Δ_{PB} and the power P of the polarizing beam and τ the total duration of the polarization process.

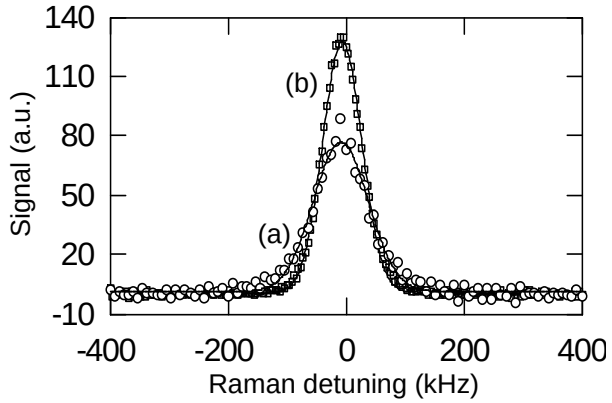

Figure 7: Counterpropagating-beam, velocity-sensitive Raman spectra. (a) Spectrum obtained with atomic polarization on the $m_4 = 0$ line (empty circles); (b) spectrum obtained with active compensation of the magnetic field (empty squares). Both lines are well fitted by Gaussians, from which one deduces temperatures of, resp., 23 and 16 T_r, (4.6 and 3.2 μK). For comparison, the recoil velocity corresponds to $\sim$ 8 kHz of Raman detuning.

Table I displays the parameters used and the observed linewidths. As expected, using a back-reflected PB produces a minimum of heating for a detuning of -0.5Γ, corresponding to the minimum temperature of the Doppler cooling, producing an increase in the *rms* velocity of 20%, from 4.0 to 4.8 v_r.

Fig. 7 compares the spectra obtained with and without the application of the PB. They are very well fitted by Gaussians, and can be considered as directly proportional to the velocity distribution. One observes, aside the heating effect discussed above, that the ratio of the surfaces of the two distributions is $\sim$11%; the atom losses are thus rather acceptable. However, we observed an unexplained decrease of the signal to noise ratio of a factor 1.8 in the polarized case.

V. MODEL

In order to understand the polarizing process dynamics, we performed, as in ref. [12], numerical simulations based on a rate-equation approach taking into account the effect of the PB and of the repumper, that is, including all transitions considered in Fig. 1. We identify a given sublevel by three labels: $s = \{g, e\}$ characterizing fine-structure state, $F = \{3, 4, 5\}$ for the hyperfine sublevel and $m_F = \{-F...F\}$ for the Zeeman sublevel. The general form of these equations is then

$$\frac{dN_{s,F,m_F}}{dt} = \sum_{s_1,F_1,m_1} W_{s_1,F_1,m_1\to s,F,m_F} N_{s_1,F_1,m_1} - \sum_{s_1,F_1,m_1} W_{s,F,m_F\to s_1,F_1,m_1} N_{s,F,m} + \delta_{s,g} \sum_{s_1,F_1,m_1} \Gamma a_{e,F_1,m_1\to g,F,m_F} N_{g,F_1,m_1} - \delta_{s,e}\Gamma N_{e,F,m}. \quad (3)$$

where N_{s,F,m_F} is the population of the sublevel $\{s, F, m_F\}$, $W_{s,F,m_F\to s_1,F_1,m_1}$ is the stimulated transition rate between levels $\{s, F, m_F\}$ and $\{s_1, F_1, m_1\}$, and $a_{e,F_1,m_1\to g,F,m_F}$ is the spontaneous emission branching ratio connecting the sublevels $\{e, F_1, m_1\}$ and $\{g, F, m_F\}$. The first two terms describe the population and the depopulation of the sublevel by stimulated transitions, the third term describes the population of a ground-state sublevel by spontaneous emission and the last term, the depopulation of an excited level by spontaneous emission.

If we choose a reference frame with the z axis oriented along the bias magnetic field, the polarization of the beams can be expressed in terms of three unitary polarization vectors

$$\epsilon_0 = \mathbf{z} \quad (4)$$

$$\epsilon_1 = \frac{\mathbf{x} + i\mathbf{y}}{\sqrt{2}} \quad (5)$$

$$\epsilon_{-1} = \frac{\mathbf{x} - i\mathbf{y}}{\sqrt{2}} \quad (6)$$

and the generic polarization of a beam is

$$\varepsilon = \sum_{q=-1}^{1} \varepsilon_q \epsilon_q. \quad (7)$$

The absorption and stimulated emission rates $W_{s,F,m_F\to s_1,F_1,m_1}$ are related to the spontaneous emission rates $a_{e,F_1,m_1\to g,F,m_F}$ by the following relation:

$$W_{s,F,m_F\to s_1,F_1,m_1} = \frac{3}{2}\frac{\lambda_L^3}{\pi hc}\frac{I}{\Delta_L}\chi_{F\to F_1} \times a_{e,F_1,m_1\to g,F,m_F}\Gamma\varepsilon^2_{m_F-m_1} \quad (8)$$

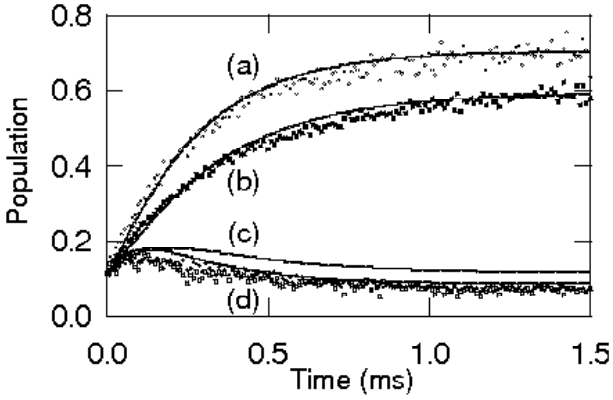

Figure 8: Dynamics of the polarization process. (a) Population of the $m_4 = 0$ level with $\Delta_{PB} = -0.5\Gamma$, (solid lines are fits by numerical simulation curves); (b) Population of the $m_4 = 0$ level with $\Delta_{PB} = 0$; (c) Population of the $m_4 = 1$ level with $\Delta_{PB} = 0$; (d) Population of the $m_4 = 1$ level with $\Delta_{PB} = -0.5\Gamma$. Parameters are $I_{PB}/I_s = 0.019$, $I_{repumper}/I_s = 0.023$, $\alpha = 0.013$.

where $\lambda_L = 852$ nm is the laser wavelength, I the laser intensity expressed in W.m^{-2} and $\Delta_L \sim 2\pi \times 1$ MHz the laser linewidth, and

$$\chi_{F\to F_1} \equiv \mu(\mu+1)\frac{\Delta^2_{F\to F_1} + (\mu-1)^2}{(\Delta^2_{F\to F_1} + \mu^2 - 1)^2 + 4\Delta^2_{F\to F_1}} \quad (9)$$

is the relative probability of exciting a neighbouring transition with $\mu = \Delta_L/\Gamma$ and $\Delta_{F\to F_1} = 2(\omega_{F\to F_1} - \omega_L)/\Gamma$ the position of the atomic linewidth from the laser line. The branching ratios $a_{e,F_1,m_1\to g,F,m_F}$ are tabulated in [12]. Applying Eq. (3) to all transitions produces a set of 43 coupled equations. We noted however that the ratio between different values of $\chi_{F\to F_1}$ can be as large as 10^4; some transitions can in practice be neglected, and one obtains very good results with only 23 equations :-).

As we indicated in subsec. IV A, the polarization of the PB is contaminated by σ^+ and σ^- components. This is taken into account in our simulation by writing its polarization as

$$\varepsilon = \frac{\epsilon_\mathbf{0} + \alpha\epsilon_+ + \alpha\epsilon_-}{\sqrt{1+2\alpha^2}} \quad (10)$$

α being an adjustable parameter representing the depolarization of the PB. The coupled rate equation are numerically solved using a standard 4$^{\text{th}}$ order Runge-Kutta integration method with the initial condition that all ground states levels $|F = 4; m_f\rangle$ are equally populated.

The results of the simulations are displayed in Fig. 8. It fits very well the experimental results, except for the population of the $m_4 = 1$ level with $\Delta_{PB} = 0$, where one observes a systematic shift. This is probably due to the fact that these small values are close to the detection level of the background correction (see sec. III). We

deduce a rather small depolarization value of $\alpha = 0.013$, which shows that the process is very sensitive to these effects. The simple approach based on rate equations thus describes well the dynamics of the polarization process.

VI. CONCLUSION

We have demonstrated the ability of the polarization technique to produce very sharp Raman lines, allowing high-resolution Raman velocimetry of laser-cooled atoms. Our results imply a velocity resolution of $v_r/50$, which corresponds to a de Broglie wavelength of $50\lambda_L$, which allows us, by performing Raman velocity-selective pulses, to potentially generate quantum-coherent spatial atomic wavefunctions extending up to 100 wells of a standing wave. This opens new perspectives for manipulating the external degrees of freedom of atoms, in the frame of experiments on quantum dynamics, specially involving quantum chaos and quantum transport in optical potentials.

Acknowledgments

Laboratoire de Physique des Lasers, Atomes et Molécules (PhLAM) is Unité Mixte de Recherche UMR 8523 du CNRS et de l'Université des Sciences et Technologies de Lille. Centre d'Etudes et de Recherches Laser et Applications (CERLA) is supported by Ministère de la Recherche, Région Nord-Pas de Calais and Fonds Européen de Développement Économique des Régions (FEDER).

[1] M. Kasevich, D. S. Weiss, E. Riis, K. Moler, S. Kasapi, and S. Chu, Phys. Rev. Lett. **66**, 2297 (1991).
[2] M. Kasevich and S. Chu, Phys. Rev. Lett. **69**, 1741 (1992).
[3] V. Boyer, L. J. Lising, S. L. Rolston, and W. D. Phillips, Phys. Rev. A **70**, 043405 (2004).
[4] V. Vuletic, C. Chin, A. J. Kerman, and S. Chu, Phys. Rev. Lett. **81**, 5768 (1998).
[5] M. Morinaga, I. Bouchoule, J. C. Karam, and C. Salomon, Phys. Rev. Lett. **83**, 4037 (1999).
[6] J. Ringot, P. Szriftgiser, J. C. Garreau, and D. Delande, Phys. Rev. Lett. **85**, 2741 (2000).
[7] I. Dotsenko, W. Alt, S. Kuhr, D. Schrader, M. Müller, Y. Miroshnychenko, V. Gomer, A. Rauschenbeutel, and D. Meschede, App. Phys. B **78**, 711 (2004).
[8] P. Cladé, E. de Mirandes, M. Cadoret, S. Guellati-Khélifa, C. Schwob, F. Nez, L. Julien, and F. Biraben, Phys. Rev. Lett. **96**, 033001 (2006).
[9] Shielding against magnetic field fluctuations can be achieved by a physical "μ-metal" shielding or by an electronic feedback-loop active compensation [11].
[10] Throughout this paper we use the following conventions to note Zeeman sublevels: ground state sublevels are noted F,m_F and excited-state sublevels are noted F',$m_{F'}$.
[11] J. Ringot, P. Szriftgiser, and J. C. Garreau, Phys. Rev. A **65**, 013403 (2002).
[12] G. Avila, V. Giordano, V. Candelier, E. de Clercq, G. Theobald, and P. Cerez, Phys. Rev. A **36**, 3719 (1987).
[13] H. Perrin, A. Kuhn, I. Bouchoule, T. Pfau, and C. Salomon, Europhys. Lett. **46**, 141 (1999).
[14] J. Ringot, Y. Lecoq, J. C. Garreau, and P. Szriftgiser, Eur. Phys. J. D **7**, 285 (1999).